

# 1    **The relationship between mantle pH and the deep nitrogen cycle**

2    Sami Mikhail<sup>1,2</sup>, Peter H. Barry<sup>2</sup>, Dimitri A. Sverjensky<sup>3</sup>

3    <sup>1</sup>*The School of Earth and Environmental Sciences, The University of St. Andrews, St. Andrews, UK, email: [sm342@st-](mailto:sm342@st-andrews.ac.uk)*  
4    *[andrews.ac.uk](mailto:sm342@st-andrews.ac.uk)*

5    <sup>2</sup>*St Andrews Centre for Exoplanet Science, The University of St. Andrews, UK*

6    <sup>3</sup>*The Department of Earth Sciences, The University of Oxford, Oxford, UK*

7    <sup>4</sup>*The Department of Earth and Planetary Sciences, Johns Hopkins University, Baltimore, M.D., USA*

## 8    **Abstract**

9    Nitrogen is distributed throughout all terrestrial geological reservoirs (i.e., the crust, mantle, and  
10    core), which are in a constant state of disequilibrium due to metabolic factors at Earth's surface,  
11    chemical weathering, diffusion, and deep N fluxes imposed by plate tectonics. However, the  
12    behavior of nitrogen during subduction is the subject of ongoing debate. There is a general  
13    consensus that during the crystallization of minerals from melts, monatomic nitrogen behaves like  
14    argon (highly incompatible) and ammonium behaves like potassium and rubidium (which are  
15    relatively less incompatible). Therefore, the behavior of nitrogen is fundamentally underpinned by  
16    its chemical speciation. In aqueous fluids, the controlling factor which determines if nitrogen is  
17    molecular (N<sub>2</sub>) or ammoniac (inclusive of both NH<sub>4</sub><sup>+</sup> and NH<sub>3</sub><sup>0</sup>) is oxygen fugacity, whereas pH  
18    designates if ammoniac nitrogen is NH<sub>4</sub><sup>+</sup> and NH<sub>3</sub><sup>0</sup>. Therefore, to address the speciation of nitrogen  
19    at high pressures and temperatures, one must also consider pH at the respective pressure–  
20    temperature conditions. To accomplish this goal we have used the Deep Earth Water Model  
21    (DEW) to calculate the activities of aqueous nitrogen from 1-5 GPa and 600-1000 °C in equilibrium  
22    with a model eclogite-facies mineral assemblage of jadeite + kyanite + quartz/coesite  
23    (metasediment), jadeite + pyrope + talc + quartz/coesite (metamorphosed mafic rocks), and  
24    carbonaceous eclogite (metamorphosed mafic rocks + elemental carbon). We then compare these  
25    data with previously published data for the speciation of aqueous nitrogen across these respective  
26    P-T conditions in equilibrium with a model peridotite mineral assemblage (Mikhail, S. Sverjensky,  
27    D.A. 2014. *Nature. Geoscience* 7, 816–819). In addition, we have carried out full aqueous  
28    speciation and solubility calculations for the more complex fluids in equilibrium with jadeite +  
29    pyrope + kyanite + diamond, and for fluids in equilibrium with forsterite + enstatite + pyrope +  
30    diamond.

31    Our results show that the pH of the fluid is controlled by mineralogy for a given pressure and  
32    temperature, and that pH can vary by several units in the pressure-temperature range of 1-5 GPa

and 600-1000 °C. Our data show that increasing temperature stabilizes molecular nitrogen and increasing pressure stabilizes ammoniac nitrogen. Our model also predicts a stark difference for the dominance of ammoniac vs. molecular and ammonium vs. ammonia for aqueous nitrogen in equilibrium with eclogite-facies and peridotite mineralogies, and as a function of the total dissolved nitrogen in the aqueous fluid where lower N concentrations favor aqueous ammoniac nitrogen stabilization and higher N concentrations favor aqueous N<sub>2</sub>.

Furthermore, we present thermodynamic evidence for nitrogen to be reconsidered as an extremely dynamic (chameleon) element whose speciation and therefore behavior is determined by a combination of temperature, pressure, oxygen fugacity, chemical activity, and pH. We show that altering the mineralogy in equilibrium with the fluid can lead to a pH shift of up to 4 units at 5 GPa and 1000 °C. Therefore, we conclude that pH imparts a strong control on nitrogen speciation, and thus N flux, and should be considered a significant factor in high temperature geochemical modeling in the future. Finally, our modelling demonstrates that pH plays an important role in controlling speciation, and thus mass transport, of Eh-pH sensitive elements at temperatures up to at least 1000 °C.

## 1. INTRODUCTION

Nitrogen is the dominant gas in Earth's atmosphere and is distributed in all terrestrial geological reservoirs, which are in a constant state of disequilibrium (see Busigny & Bebout, 2013; Bebout et al., 2013, 2016; Johnson & Goldblatt, 2015). The flux of nitrogen between the surface and interior is governed by volcanism (out-gassing) and subduction (in-gassing); this interplay ultimately controls atmospheric N<sub>2</sub> levels (see discussion in Barry & Hilton, 2016), which are intimately linked with biology (Stüeken et al., 2016; Zerkle & Mikhail, 2017). But to constrain the N flux and/or the partial pressure of atmospheric N over geologically-long (>Ga) timescales is difficult due to a lack of samples (e.g. Marty et al., 2013; Som et al., 2012; 2016). Consequently, in order to address these issues, workers must combine the evidence from sparse deep-time N datasets with experimental and theoretical (thermodynamic) models to estimate past nitrogen dynamics.

At present, there is no consensus for the direction (i.e., positive or negative ) or magnitude of the global N flux out of the Earth through time (Dauphas & Marty, 1999; Fischer et al., 2002; Marty & Dauphas, 2003; Busigny et al., 2003; Elkins et al., 2006; Philippot et al., 2007; Yokochi et al., 2009; Mohapatra et al., 2009; Halama et al., 2010, 2014; Palot et al., 2012; Mikhail et al., 2014; Mikhail & Sverjensky, 2014; Barry & Hilton, 2016; Zerkle & Mikhail, 2017). As a result, there is no

quantitative explanation for the discrepancy between calculated N-fluxes from different arc systems (see recent reviews by Busigny & Bebout, 2013; Bebout et al., 2013, 2016), and thus the nature of the deep nitrogen cycle remains a controversial topic (Zerkle & Mikhail, 2017).

To understand the pathways followed by N during subduction requires a first-order understanding of the partitioning behavior of nitrogen within specific minerals. For example, molecular nitrogen ( $\text{N}_2^0$ ) and ammonia ( $\text{NH}_3^0$ ) are both neutrally charged, and therefore highly incompatible in most mineral phases (Brooker et al., 2003). Conversely, ammonium ( $\text{NH}_4^+$ ) is positively charged and has an ionic radius between those of  $\text{Rb}^+$  and  $\text{K}^+$ , and thus should be compatible in K-bearing phases such as phengite, phlogopite, K-bearing clinopyroxene, K-hollandite, Phase-X ((K) $\text{Mg}_2\text{Si}_2\text{O}_7\text{H}$ ) (Honma & Itihara, 1983; Haendel et al., 1986; Busigny et al., 2003; Yokochi et al., 2009; Palya et al., 2011; Bebout et al., 2016). Ammonium has also been shown to dissolve as a trace component in K-absent mafic minerals (Li et al., 2013; Watenphul et al., 2010). Therefore, the behavior of nitrogen is predictably governed by the speciation of nitrogen where neutrally charged compounds are – thermodynamically speaking – highly incompatible (Blundy & Wood, 2003), an assertion that has been demonstrated experimentally (Brooker et al., 2003).

For high temperature aqueous systems, the speciation of N has been constrained as a function of oxygen fugacity (Mikhail & Sverjensky, 2014; Li & Keppler, 2014), and both studies agree that most nitrogen in upper mantle fluids should be ammoniac. The difference between these datasets is the nature of the ammoniac nitrogen present. For example, at 5 GP, 1000 °C, and an oxygen fugacity of -1 log units relative to the Quartz-Fayalite-Magnetite buffer reaction (QFM) the speciation of nitrogen in equilibrium with olivine ( $\text{Fo}_{90}$ ) was determined to be ammonia in quenched run products (using FTIR; Li & Keppler, 2014), but the predicted speciation of nitrogen in equilibrium with forsterite + enstatite is ammonium (Mikhail & Sverjensky, 2014). We note that this could be the result of quenching, where ammonium (a reactive ion) re-equilibrates to a stable state during cooling (pre-analysis). But the controlling factor, which designates if ammoniac nitrogen is  $\text{NH}_4^+$  and  $\text{NH}_3^0$  is not oxygen fugacity, but rather pH – and more alkaline conditions favor  $\text{NH}_3^0$ . This implies that the pH of the fluid in equilibrium with olivine ( $\text{Fo}_{90}$ ; Li and Keppler, 2014) may be more alkaline than is predicted for pH of the fluid in equilibrium with forsterite + enstatite (where pH can be expressed as proportional to  $\log[\text{Mg}^{2+}/(\text{H}^+)^2]$ ; Mikhail and Sverjensky, 2014). Overall, this result implies pH is a significant variable at high temperatures.

Here we investigate the effect of pH on the speciation of nitrogen under upper mantle P-T- $f\text{O}_2$  conditions as a function of system stoichiometry using a hypothetical host-rock mineralogy. As is

the case with  $fO_2$ , the pH of the system is governed by pressure, temperature and composition (P-T-X). In the case of nitrogen geochemistry for our study, this can be considered as the equilibrium between a fluid and a solid, therefore if all else is equal, the stoichiometry of the system can exert control on the pH and therefore the speciation and behavior of nitrogen. This is because different protonation reactions can buffer the pH of the fluid to different values (e.g., whether the protonation reactions are governed by the  $\log[\alpha Mg^{2+}/(\alpha H^+)^2]$  or  $\log[\alpha Na^+/\alpha H^+]$ ). Herein we investigate the role of a hypothetical mineralogy (for stoichiometry) on fluid pH by presenting the outputs from a series of thermodynamic calculations, and we discuss the implications of our findings in light of the deep-Earth nitrogen cycle, and mantle geochemistry.

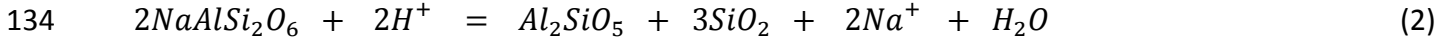
106

## 107 2. METHODS

The speciation of aqueous ions, metal complexes, neutral species and minerals can be predicted by applying the Helgeson-Kirkham-Flowers (HKF) equations of state (Helgeson and Kirkham, 1974a,b, 1976; Helgeson et al., 1981; as revised in Tanger and Helgeson, 1988, and Shock and Helgeson, 1988). Prior to recent pioneering work (Pan et al., 2013; Facq et al., 2014; Sverjensky et al., 2014a) there was a historic limitation of pressure  $< 0.5$  GPa, due to the fact that the dielectric constant of water was not known at higher pressures (Johnson et al., 1992; Shock et al., 1992). This precluded the application of the HKF equations of state to matters concerning aqueous fluids in deep Earth systems (e.g., lower crust, upper mantle, and subduction zones). However, the dielectric constant of water has recently been constrained  $\leq 6$  GPa (Sverjensky et al., 2014a), which enables an extension of the P-T range for the application of the HKF equations of state for aqueous species up to  $\leq 6$  GPa and  $\leq 1200^\circ\text{C}$  (Pan et al., 2013; Facq et al., 2014; Sverjensky et al., 2014a). As a result, it is now feasible to determine the speciation of aqueous ions, metal complexes, neutral species and minerals across conditions akin to the pressure and temperature pathway followed by a subducted-slab from Earth's surface to a depth of approximately 150 km using the Deep Earth Water (DEW) model. As previously described (Sverjensky et al., 2014b; Sverjensky & Huang, 2015; Mikhail & Sverjensky, 2014), the DEW model enables calculation of equilibrium constants involving aqueous species of all kinds as a function of temperature and pressure, and the incorporation of these equilibrium constants into aqueous speciation, solubility, and chemical mass transfer codes.

We have predicted the speciation of nitrogen as a function of P-T- $fO_2$ -pH. Note, pH is a function of the activities of  $Mg^{2+}$  and  $Na^+$  in supercritical aqueous fluid in equilibrium with specific mineral

assemblages (Sverjensky et al., 2014). The pH values denoted by subducted oceanic crust in **Figs. 1a-d** were constrained by equilibrium with the model eclogite-facies mineral assemblages (jadeite + kyanite + SiO<sub>2</sub> representing metasediment, and jadeite + pyrope + talc + SiO<sub>2</sub> representing metamorphosed mafic rocks) at pressures of 1 and 5 GPa and temperatures of 600 to 1,000°C. The equilibrium between fluid and jadeite, kyanite, SiO<sub>2</sub> enables derivation of the following equations:

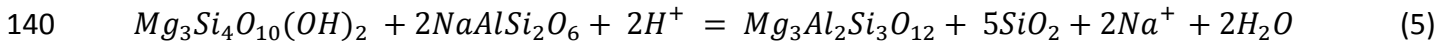


$$\text{for which} \quad \log K_2 = \log \frac{a_{Na^+}^2}{a_{H^+}^2} \quad (3)$$

Assuming pure minerals and unit activities of the minerals and the water results in

$$pH = \frac{1}{2} \log K_2 - \log a_{Na^+} \quad (4)$$

For the mafic eclogite-facies mineral assemblages, equilibrium between the components of jadeite, garnet, talc and SiO<sub>2</sub> enables writing



$$\text{for which} \quad pH = \frac{1}{2} \log K_5 - \log a_{Na^+} \quad (6)$$

Noteworthy, SiO<sub>2</sub> is coesite at 5 GPa (600 & 1000 °C), but at 1 GPa SiO<sub>2</sub> is stable as either α-Qtz (600 °C) and β-SiO<sub>2</sub> (1000 °C). A range of values for the  $a_{Na^+}$  from 0.01 to 1.0 were used in Eqns. (4) and (6) resulting in a range of estimated pH values. For example, at 5 GPa and 600 °C, the calculated pH values from Eqns. 4 and 6 are 3.1 - 5.1 and 3.2 - 5.2, for metasedimentary and mafic eclogites respectively. Because these two ranges are indistinguishable on this scale, we only plot the values from Eqn. 4 in **Figs. 1a-d** (subducted oceanic crust). The assumption of pure minerals introduces small uncertainties on the scale of the plots shown. For example, a decrease in the activity of jadeite in Eqn. (4) from 1.0 to 0.5 would produce a decrease in the pH in Eqn. (6) of 0.30, which is relatively small compared to the range of Na<sup>+</sup> activities assumed. Very low activities of jadeite would produce a bigger effect (e.g., if the activity of jadeite were reduced from 1.0 to 0.10, the pH would be decreased by 1.0 unit). Furthermore, by applying values of logK calculated as described above, together with the range of activities for the Mg<sup>2+</sup> and Na<sup>+</sup> corresponds to a range of pH values for the fluids. It should be emphasized that uncertainties caused by using the pure minerals and water are rather small on a logarithmic scale such as in **Figs. 1a-d** compared to the range of pH associated with the range of activities for either Mg<sup>2+</sup> or Na<sup>+</sup>.

157 The boundaries between the various nitrogen species shown in **Figs. 1a-d** depend on the  
158 stoichiometry of the equilibria, the magnitudes of the relevant equilibrium constants, and the  
159 total dissolved nitrogen (Mikhail and Sverjensky, 2014). The latter dependence is a consequence of  
160 equilibria between  $N_2$ , which has two moles of N, and reduced N-species, which have one mole of  
161 N in each. As a consequence, the speciation of N in aqueous fluids at equilibrium is a function of  
162 the total dissolved nitrogen in the fluid. In our calculations, we consider a large range of possible  
163 nitrogen concentrations from 0.001 to 1 m N, corresponding to concentrations between 14 ppm  
164 by mass and 1.4 wt.%. This range was selected in order to simulate a wide range of likely fluid  
165 compositions that might be found in nature, but also to constrain the effect of N concentration  
166 (order of magnitude scales).

167 Although nitrogen concentrations in aqueous fluids from the upper mantle are poorly known  
168 (because aqueous fluids from the upper mantle are rarely sampled), the concentrations in  
169 minerals are better constrained. We cite a range of nitrogen concentrations measured in mantle  
170 rocks and minerals to demonstrate the possibility that aqueous fluids in the mantle might also  
171 exhibit a wide range of nitrogen concentrations. For example, typical measurements of volcanic  
172 xenoliths and basaltic samples are approximately 0.1-10 ppm by mass (whole rock from Marty,  
173 1995, mineral separates from Fischer et al., 2005; basaltic glasses from Barry et al., 2012), and the  
174 phlogopites ranges from 7.6 to 25.7 ppm by mass (Yokochi et al., 2009) and lithospheric and  
175 sublithospheric diamonds contain between <1 to >10,000 ppm by mass N (Smart et al., 2011;  
176 Mikhail et al. 2014). In fact, some very rare mantle xenoliths and diamonds contain fluid-inclusions  
177 of pure  $N_2$  (Andersen et al., 1995; Smith et al. 2014). Despite the fact that nitrogen is a trace  
178 component in material from shallow depths, typically sampled by volcanoes (see Johnson and  
179 Goldblatt et al., 2016 for a review), there are processes (i.e. metasomatism and melting) that can  
180 generate localized nitrogen-enrichment and render nitrogen a major volatile element in the  
181 mantle. Therefore, the concentrations used here (ca. 14 ppm by mass to 1.4 wt.%) are not  
182 unrealistic, and enable us to investigate the speciation of nitrogen as a function of P, T,  $fO_2$ , pH,  
183 and nitrogen concentration.

184

### 185 **3. RESULTS**

186 Superposed on **Figs. 1a-d** are fields representing the calculated (theoretical and empirical) oxygen  
187 fugacities of peridotitic (Woodland et al. 1992; 1996, 2006; Ionov & Wood 1992; Wood & Virgo  
188 1989, Canil et al. 1990, Brandon & Draper 1996, Frost and McCammon, 2008) and eclogitic rocks

189 (Simakov, 2006; Stagno et al., 2015) as well as the predicted range of pH values for aqueous fluids  
190 in equilibrium with hypothetical mineral assemblages representing model peridotite (from Mikhail  
191 & Sverjensky, 2014) and eclogite-facies mineral assemblages (this study).

192 The oxygen fugacities for peridotites in arc-mantle wedges (QFM to QFM + 2) vs. the oxygen  
193 fugacity of peridotites from sub-cratonic lithospheric mantle (QFM to QFM -3) are taken from  
194 Frost and McCammon (2008). The available data suggest eclogitic rocks cover a similar  $fO_2$  range  
195 to their peridotitic counterparts (Simakov, 2006; Stagno et al., 2015; Smart et al., 2016). We plot a  
196 larger range for the  $fO_2$  of eclogites in the **figures** (QFM to QFM - 4) to account for the observed  
197 occurrence of carbides, nitrides and native metals in samples from the obducted Tibetan  
198 ophiolites ( $\leq$  QFM - 4; Dobrzhinetskaya et al., 2009). In addition, the sediments subducted beneath  
199 the Cyclades Greek islands are relatively oxidized ( $\geq$  QFM - 1; Ague and Nicolescu, 2014), having  
200 stable carbonate phases. The range of  $fO_2$  values for eclogites shown in **Figs. 1a-d** represents the  
201 global range, and is not intended to represent any single geographical locality (i.e., data from  
202 Tibetan and Greek obducted rocks are provided to illustrate the large range of  $fO_2$  values in  
203 measured subducted assemblages).

204 The pH values plotted here correspond to the calculated equilibrium between water and pure  
205 forsterite + enstatite (model peridotite – Mikhail & Sverjensky, 2014) and hypothetical eclogite-  
206 facies mineral assemblages; jadeite + kyanite +  $SiO_2$  (metasediment – this study), jadeite + pyrope  
207 + talc +  $SiO_2$  (metamorphosed mafic rocks – this study), and carbonaceous eclogite-facies mineral  
208 assemblages (metamorphosed mafic rocks + elemental carbon; this study). Importantly, the  
209 relative proportions of the pure minerals do not influence the fluid chemistry, because the fluid  
210 chemistry is set by the equilibrium constants (see methods). In our model, pH is expressed by the  
211  $a_{H^+}$  (fluid) and  $a_{Na^+}$  (eclogite – this study) and  $a_{Mg^{2+}}$  (peridotite; Mikhail & Sverjensky, 2014) (eq.4  
212 and eq.6). We have applied a range of activities for  $a_{Na^+}$  and  $a_{Mg^{2+}}$  from 0.1 to 1 (e.g. eq.3). Our  
213 calculations show the speciation of aqueous ammoniac nitrogen in equilibrium with eclogite-facies  
214 metasediments and mafic rocks (herein collectively referred to as eclogite-facies mineral  
215 assemblage; this study) is predicted to differ from aqueous nitrogen in equilibrium with  
216 peridotites under most of the conditions investigated (**Figs. 1a-d**). Under most conditions,  
217 ammonium ( $NH_4^+$ ) dominates in peridotite, and ammonia ( $NH_3^0$ ) is dominant in the eclogite-facies  
218 mineral assemblages; this is due to the eclogite-facies mineral assemblages buffering the fluid to  
219 higher pH conditions (**Figs. 1a-d**).

220 For an oxygen fugacity of QFM -1 to -2, 600°C, and 1 or 5 GPa (**Figs 1a and 1c** respectively), the  
221 dominant nitrogen species in the fluid are predicted to be  $\text{NH}_3^0$  or  $\text{NH}_4^+$ , depending on pressure  
222 and pH. At 1,000°C and 1 or 5 GPa (**Figs 1b and 1d** respectively), the dominant nitrogen species in  
223 the fluid is predicted to be  $\text{N}_2^0$ . This temperature range is relevant to modern arc systems. For  
224 example, Syracuse et al., (2010) calculated the thermal models for 204 slab temperatures in arc  
225 systems on the Pacific rim and found the range to be 301 to 987°C, with a mean of  $789 \pm 76^\circ\text{C}$ .  
226 Thus, our results strongly suggest that the nitrogen speciation in eclogitic fluids in 'cold'  
227 subduction zones differs from those in 'hot' subduction zones. Note, the exact thermal regimes for  
228 hot and cold subduction zones are difficult to constrain, because there are a number of dependent  
229 and independent variables to consider which control the thermal-depth status of a subducted slab  
230 (age of slab, slab-dip, slab T beneath arc, Moho T beneath arc, velocity of subduction) and the  
231 temperature also varies significantly with distance from slab surface (in both directions; Syracuse  
232 et al., 2010). Furthermore, because geothermal gradients during subduction are non-linear, there  
233 are multiple degrees of freedom to explore. To examine this further, we direct the reader to  
234 Syracuse et al. (2010). Herein, we refer to cold subduction zones as those with a thermal gradient  
235 (at the slab surface) of  $<10^\circ\text{C/km}$ .

236 A significant difference between cold and hot subduction regimes are shown more distinctly in  
237 **Figs.2a-b & 3a-b**. We calculated a full aqueous speciation model at 5.0 GPa between 600 and  
238 1,000°C at QFM - 2 for aqueous nitrogen in fluids in equilibrium with a model eclogite consisting of  
239 jadeite + pyrope + kyanite + coesite, +diamond and a model peridotite consisting of forsterite +  
240 enstatite + pyrope + diamond. The latter is a more complex chemical system than has previously  
241 been considered (Mikhail & Sverjensky, 2014). Results are shown for high ( $0.1 \text{ m N} \approx 1.4 \text{ wt\% N}$ )  
242 and low ( $0.001 \text{ m N} \approx 14 \text{ ppm by mass N}$ ) nitrogen concentrations. Unreactive aqueous nitrogen  
243 ( $\text{N}_2^0 + \text{NH}_3^0$ ) progressively increase in N concentration and then dominate over reactive nitrogen  
244 ( $\text{NH}_4^+$ ) in fluids in equilibrium with the eclogite-facies assemblage while temperature increases  
245 from 600-1000°C (**Fig.2a-b**). For the model peridotite assemblage the relationship is similar for  
246 high nitrogen concentrations, where molecular aqueous nitrogen ( $\text{N}_2$ ) progressively increases in  
247 abundance and then dominates over reactive nitrogen ( $\text{NH}_4^+$ ), but importantly, ammonia is always  
248 less dominant than what we find for the eclogite-facies eclogites assemblage (**Fig.3b**). However,  
249 for low N concentrations in equilibrium with the peridotite assemblage, ammonium is the most  
250 abundant species across all temperatures investigated (**Fig.3a**). Therefore, the hottest subduction  
251 zone fluids at QFM-2 are predicted to be dominated by  $\text{N}_2$  at higher N concentrations in both  
252 eclogite-facies (**Fig.2b**) and model peridotite (**Fig.3b**) assemblages, but at the lowest N-



253 concentrations, N<sub>2</sub> is minor for both eclogite (**Fig.2a**) and peridotite (**Fig.3a**) with ammonia and  
254 ammonium dominating, respectively. Note, the difference in domination for ammonia and  
255 ammonium between the eclogite and peridotite simulations is the function of differing pH values  
256 for the fluids at high temperatures (**Fig.1**).

257

## 258 **4. DISCUSSION**

### 259 **4.1 Limitations of the approach**

260 This study examines the role of pH in the deep-Earth nitrogen cycle at temperatures from 400-  
261 1000°C and pressures of 1-5 GPa (**Figs. 1-3**). We have calculated the pH for aqueous fluids in  
262 equilibrium with hypothetical eclogite-facies and metasediments with a simple bulk chemistry.  
263 However, our approach does not consider some important and classically considered electron-  
264 donor elements (i.e., Fe<sup>2+,3+</sup>, S<sup>-2,+6</sup>) nor do we consider the role of alkali metals besides Na<sup>+</sup> (K<sup>+</sup>,  
265 Rb<sup>+</sup>, Cs<sup>+</sup>). Furthermore, under water-saturated conditions at 1000 °C and 1 GPa, peridotites and  
266 eclogites would likely melt (Grove et al., 2006). The DEW model does not (presently) take melting  
267 into account, and therefore we can only show the predicted speciation of aqueous nitrogen in  
268 equilibrium with solid mineral phases. If a melt phase were present, the partitioning of ions could  
269 be affected, and therefore the pH values of the aqueous fluids could also be affected. Therefore,  
270 we acknowledge that our approach represents a simplification. Nonetheless, our approach does  
271 allow for robust constraints to be applied based on the effect of pH on the speciation of aqueous  
272 nitrogen at high temperatures and pressures. The modeling detailed here shows how changes in  
273 pH as a function of mineralogy are not only possible, but are predicted to be large (orders of  
274 magnitude – **Fig.1a.d**), and this approach has been further reinforced by a recent study employing  
275 a different (theoretical) modeling approach (Galvez et al., 2016). Ergo, large changes in *f*O<sub>2</sub> are  
276 predicted, which is consistent with empirical data and conventional understanding. However, we  
277 also predict large variations in pH, which also overlap with speciation changes for nitrogen  
278 between three distinct species (NH<sub>4</sub><sup>+</sup>-NH<sub>3</sub><sup>0</sup>-N<sub>2</sub><sup>0</sup>).

279

### 280 **4.2 Ammonia and Ammonium**

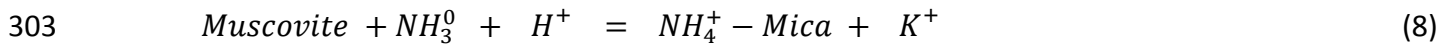
281 Our results show, that nitrogen can occur either in a neutral or positively charged state at high  
282 temperatures in the mantle, where molecular vs. ammoniac is dependent on *f*O<sub>2</sub> (i.e. Mikhail &  
283 Sverjensky, 2014), but ammonia vs. ammonium is dependent on pH (this study). For example, at

700°C, 5 GPa, and a  $\log f_{O_2} - 2$  ( $\Delta QFM$ )  $> 80\%$  of the nitrogen in equilibrium with Jadeite + Pyrope + Kyanite +  $SiO_2$  + Diamond will be at  $NH_4^+$  but neutrally charged nitrogen becomes dominant with increasing temperature, where  $NH_4^+$  drops off to 10% and  $N_2^0$  and  $NH_3^0$  make up 60 and 30 % of the fluid, respectively, at 1000°C (**Fig. 2a**). At 1000°C and 5 GPa (**Fig. 1d**), aqueous nitrogen in fluids under equilibrium with eclogite are predicted to be more alkaline than in peridotite, and there are a wide range of conditions where  $NH_3^0$  will be the dominant nitrogen species (**Fig. 1d**). As a further additional complexity influencing the behavior of nitrogen in upper mantle fluids, the total amount of nitrogen in the fluids also affects the speciation (**Figs. 2-3**). For example, in **Fig. 1a**, the speciation of nitrogen in eclogitic fluids at QFM – 2, ranges from  $NH_3^0$  in low-N fluids to  $N_2$  in high-N fluids.

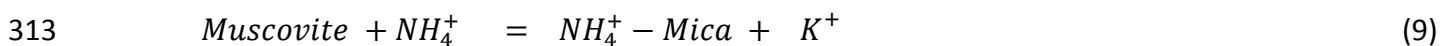
We note that the dominance of  $NH_3^0$  in our hypothetical eclogite-facies and metasediments must be considered a gross simplification for the sake of constraining the first-order level effect of pH. Nonetheless, this result can be viewed as an upper limit, where the addition of  $H^+$  would hydrolyze  $NH_3^0$  to  $NH_4^+$ . We further note that there are other reactions (in nature) which can produce  $H^+$  ions and convert  $NH_3^0$  to  $NH_4^+$ . For example, such reactions require coupling with a reaction that produces  $H^+$  ions during subduction (e.g., the carbonation of calcium shown in equation 7):



Therefore, we can model the incorporation of neutrally charged ammonia into K-bearing minerals through pH-dependent reactions such as:



Because some carbonation reactions generate  $H^+$  ions (e.g. Eq.7), the pH of fluids in equilibrium with eclogites may not inherently destabilize ammonium, but instead the stability of ammonium over ammonia in nature may depend on the bulk chemistry of the more complex natural system(s). Therefore, future empirical work may indeed link the carbon cycle with the nitrogen cycle, on a more genetic basis. To take this further requires extensive experimental and theoretical interrogation in the near future to examine the pH shift and the dramatic effect on N speciation (shown here). However, where conditions permit and ammonium is stabilized, the secondary  $H^+$ -producing reactions (e.g., Eq.7) are not required for nitrogen to exchange for potassium directly (Eq.9):



Our data also show that fluid mobilization from the sedimentary package into the mantle (eclogite or peridotite) will result in transitions between  $N_2^0$ ,  $NH_3^0$ , and  $NH_4^+$ , where the nature of these transitions will vary depending on whether or not the reaction is driven by pH,  $fO_2$ , or even the N concentration in the fluid (**Fig.2-3**). In short, the fluid pathway and bulk compositions (i.e., slab-mantle systems, slab-ambient mantle, and mantle wedge-ambient mantle) will determine the aqueous N-speciation (**Fig.1a-d**). Therefore, it is conceivable that nitrogen can behave like a highly incompatible and volatile element (e.g., a noble gas) or a large-ion lithophile element (e.g.,  $K^+$  &  $Rb^+$ ) in the same dynamic upper-mantle wedge system (see **Fig.4**). This means some arc systems can out-gas + in-gas, some will solely in-gas, and others will solely out-gas nitrogen depending upon the bulk rock geochemistry of the system. We argue that these data strongly imply that cold subduction zones favor mass transfer of N into the mantle, but hot subduction zones do not (**Fig.2**). This notion partly explains why efforts to determine a global N flux using specific geographical localities have been thwarted by contradictory (but equally correct) results (e.g., Fischer et al., 2002; Busigny et al., 2003; Elkins et al., 2006; Barry & Hilton, 2016). In fact, we argue that contrasting results should actually be expected.

In short, we propose that nitrogen should not have a single label regarding geochemical behavior. Nitrogen should not be considered lithophile, siderophile, or volatile, but instead nitrogen should always be viewed as a most dynamic *chameleon* element whose behaviour in aqueous fluids is effectively determined by a combination of temperature, pressure, oxygen fugacity, pH, and N concentration (i.e. mole fraction).

## 5. Broader Implications

### 5.1 Nitrogen Isotope Fractionation

The results discussed above have implications for the isotopic evolution of subducted nitrogen during devolatilization of the slab and/or mantle, because the magnitude and direction of  $\Delta^{15}N$  for  $NH_3^0$ - $N_2^0$ ,  $NH_4^+$ - $N_2^0$ , and  $NH_4^0$ - $NH_3^0$  differ dramatically. For example, at 600°C the predicted  $\Delta^{15}N_{NH_3-N_2}$  is -4‰,  $\Delta^{15}N_{NH_4-N_2}$  is +2‰, and  $\Delta^{15}N_{NH_4-NH_3}$  is +8‰ (Hanschmann, 1981). Therefore, the evolution of the  $\delta^{15}N$  value of subducted nitrogen cannot be modeled with a single fractionation factor ( $\Delta^{15}N$ ), because during progressive devolatilization of the slab in the mantle the magnitude and direction of  $\Delta^{15}N$  depends on upon the coupled  $fO_2$ -pH conditions for a given temperature, which should not be considered uniform across different mantle-wedge systems. Furthermore, because the stability of the K-bearing phases is a function of P-T- $X_K$ , it is unlikely to be constant with depth on a global scale (because the large P-T variability of arc systems globally; Syracuse et

al., 2010). Therefore, the magnitude and direction of  $\Delta^{15}\text{N}$  during devolatilization of nitrogen from the slab or mantle is difficult to constrain. Importantly, if the reaction in question is  $\Delta^{15}\text{N}_{\text{NH}_3-\text{N}_2}$  where the direction is for a  $^{15}\text{N}$ -depleted residuum, this may explain why some eclogitic diamonds show mantle-like negative  $\delta^{15}\text{N}$  values alongside crustal organic carbon-like light  $\delta^{13}\text{C}$  values (Cartigny et al., 1997, 1998).

## 5.2 The pH of mantle fluids

In low-temperature geochemistry, Eh and pH are both considered important variables for predicting and expressing the nature of given chemical environments (i.e., for a recent review on low-T nitrogen see Stüeken et al., 2016). Traditionally, only Eh is considered in high temperature geochemistry, and because mineral charge-balances reflect the electron exchange where most minerals receive their negative charge in the form of  $\text{O}^-$  anions, this parameter is commonly expressed as the fugacity of oxygen ( $f\text{O}_2$ ). Furthermore, traditional models for the speciation of volatile elements in mantle fluids have long been constructed based on mixtures of neutral gases ( $\text{CO}_2$ ,  $\text{CH}_4$ ,  $\text{H}_2$  and  $\text{H}_2\text{O}$ ; commonly termed COH-fluids; e.g. Zhang & Duan, 2009). Thus, the role of dissolved aqueous ions or species derived from silicate rock components have been overlooked or ignored (see Sverjensky & Huang, 2015). Because oxygen fugacity is considered of primary importance there have been numerous theoretical and empirical approaches to predicting and quantifying the fugacity of oxygen in the mantle during accretion and differentiation (Wade and Wood, 2005; Wood et al., 2006; Frost et al., 2008), in upper mantle peridotites (Wood & Virgo 1989; Woodland et al. 1992; 1996, 2006; Ionov & Wood 1992; Canil et al. 1990; Brandon & Draper 1996; Cottrell and Kelley, 2013; Rohrbach et al., 2007), lower mantle peridotites (Frost et al., 2004), in eclogites (Simakov, 2006; Stagno et al., 2015; Smart et al., 2016), in the mantle wedge of arc systems (Lecuyer and Ricard, 1999; Parkinson and Arculus, 1999; Wood, et al., 1990), and within other telluric bodies in the Solar System (Herd, 2008).

DEW model predictions now suggest pH should also be considered a significant dimension in high temperature mineralogical composition and mantle geochemistry (Sverjensky et al., 2014b; Sverjensky & Huang, 2015; Mikhail & Sverjensky, 2014; and this study), although other modeling approaches are being pioneered that have lead to the same conceptual conclusion (Galvez et al., 2016). In hindsight, the importance of high temperature pH is not a surprising result. It is well established that at lower temperatures (< ca. 400 °C) fluid-rock interaction can exert large shifts in fluid pH, which can have dramatic effects. For example, pH as a variable has been explored by experimental means to understand why some economically viable REE deposits show significant

378 REE fractionation leading to economically viable HREE-enrichment (Migdisov et al., 2009; Williams-  
379 Jones et al., 2012).

380 The most important finding of this contribution is the expected variability of the pH values of fluids  
381 in equilibrium with peridotite- and eclogite-facies assemblages across several units, even for  
382 temperatures up to 1000 °C (**Fig.1b & d**). In the case of carbon (Sverjensky et al., 2014b; Galvez et  
383 al., 2016) and nitrogen (this study) the large pH shift as a function of mineral chemistry will  
384 significantly affect the speciation and behaviour of these important elements (in the mantle and in  
385 subduction zones), and should therefore have influenced which species of pH sensitive  
386 compounds were and are degassed into planetary surface environments. Finally, our theoretical  
387 study raises several pressing questions:

388 [1] Is there stratification of aqueous fluid pH with depth in the bulk silicate Earth following  
389 pressure effects on  $\text{Mg}^{2+}/\text{Na}^{+}$  phase equilibria and phase transitions (coesite- $\alpha$ -Qtz- $\beta$ - $\text{SiO}_2$ ; Fig.1a-  
390 b)?

391 [2] How much (if at all) has the pH of aqueous mantle fluids changed through time?

392 [3] How does the pH of aqueous mantle fluids vary between the different inner solar system  
393 planets (as is the case for  $f\text{O}_2$ )?

394 [4] How accurate is the large pH shift as a function of mineralogical composition predicted in this  
395 study (**Fig.1a-d**)?

396 [5] Which reactions or elemental fractionations can be used to retrospectively constrain the pH of  
397 a metasomatized high temperature environment using data from silicate/oxide minerals or melt  
398 inclusions?

399

## 400 **6. CONCLUSIONS**

401 We have calculated the speciation of aqueous nitrogen in equilibrium with a model eclogite-facies  
402 mafic mineral assemblage and a model carbonaceous eclogite-facies mafic mineral assemblage  
403 using the DEW model. We find nitrogen to be an extremely dynamic element whose speciation  
404 and behaviour is determined by a combination of temperature, pressure, oxygen fugacity, N  
405 concentration, and pH. Our modeling results show that increasing temperature stabilizes  
406 molecular nitrogen and increasing pressure stabilizes ammoniac nitrogen – but the nitrogen  
407 concentration also exerts a governing control (**Figs.2-3**). These show that the pH of aqueous fluids  
408 is controlled by mineralogy for a given pressure and temperature and can vary by up to 4 units at 5

409 GPa and 1000 °C (**Fig.1**). This finding clearly demonstrates that pH plays an important role in  
410 controlling speciation, and thus mass transport, of Eh-pH sensitive elements (such as nitrogen) up  
411 to at least 1000 °C.

412

## 413 **Acknowledgements**

414 SM is grateful to the Carnegie Institution of Washington for funding this work through the  
415 bestowment of a Carnegie Postdoctoral Fellowship. SM also acknowledges the School of Earth and  
416 Environmental Science (St Andrews) for providing a start-up fund which assisted in the  
417 development of these data. DAS is grateful to grants from the Sloan Foundation through the Deep  
418 Carbon Observatory (Reservoirs and Fluxes, and Extreme Physics and Chemistry programs) and a  
419 community-building Officer Grant from the Sloan Foundation, as well as support from NSF grants  
420 EAR-1624325 and ACI-1550346, and a grant from the W.M. Keck Foundation (The Co-Evolution of  
421 the Geo- and Biosphere) Grant #10583-02 to Sverjensky. PHB's contribution was supported in part  
422 by the NSF grant EAR-1144559 (A Petrological and N Isotope Study Of Crustal Recycling Through  
423 Time). We wish to acknowledge discussions with David Hilton and Tobias Fischer which assisted  
424 the development of this contribution. We also wish to thank Associate Editor Prof Horst Marschall,  
425 Dr Ralf Halama (Keele University) and two anonymous reviewers for their thoughtful comments  
426 and criticisms which improved the overall quality of this manuscript.

427

## 428 **References Cited:**

- 429 Ague, J.J., Nicolescu, S. 2014. Carbon dioxide released from subduction zones by fluid-mediated  
430 reactions. *Nature Geoscience*. 7, 355–360
- 431 Andersen, T., Burke, E.A.J., Neumann, E. 1995. Nitrogen-rich fluid in the upper mantle: fluid  
432 inclusions in spinel dunite from Lanzarote, Canary Islands. *Contributions to Mineralogy and  
433 Petrology*. 120, 20-28
- 434 Barry, P.H., Hilton, D.R., Halldórsson, S.A., Hahm, D., & Marti, K. 2012. High precision nitrogen  
435 isotope measurements in oceanic basalts using a static triple collection noble gas mass  
436 spectrometer. *Geochemistry, Geophysics, Geosystems*. 13(1).
- 437 Barry, P.H., Hilton, D.R. 2016. Release of subducted sedimentary nitrogen throughout Earth's  
438 mantle. *Geochemical Perspectives Letters*. 2, 148-159
- 439 Bebout, G.E., Fogel, M.L., Cartigny, P. 2013. Nitrogen: Highly volatile yet surprisingly compatible.  
440 *Elements*. 9, 333-338
- 441 Bebout, G., Lazzeri, K., Geiger, C.A. 2016. Pathways for nitrogen cycling in Earth's crust and upper  
442 mantle: A review and new results for microporous beryl and cordierite. *American Mineralogist*,  
443 101, 7-24.

444 Blundy, J., Wood, B.J. 2003 Partitioning of trace elements between crystals and melts. *Earth and*  
 445 *Planetary Science Letters*, 210, 383–397

446 Brandon A.D, Draper D.S. 1996. Constraints on the origin of the oxidation state of mantle overlying  
 447 subduction zones: an example from Simcoe, Washington, USA. *Geochimica Cosmochimica et Acta*,  
 448 60, 1739–1749

449 Brooker, R.A., Du, Z., Blundy, J., Kelley, S.P., Allan, N.L., Wood, B.J., Chamorro, E.M., Wartho, J.A.,  
 450 Purton, J.A. 2003. The ‘zero charge’ partitioning behaviour of noble gases during mantle melting.  
 451 *Nature*, 423 738–741

452 Busigny, V., Bebout, G.E. 2013. Nitrogen in the silicate Earth: Speciation and isotopic behaviour  
 453 during mineral-fluid interactions. *Elements*, 9, 353–358

454 Busigny, V., Cartigny, P., Philippot, P., Ader, M., Javoy, M. 2003. Massive recycling of nitrogen and  
 455 other fluid-mobile elements (K, Rb, Cs, H) in a cold slab environment: evidence from HP to UHP  
 456 oceanic metasediments of the Schistes Lustrés nappe (western Alps, Europe). *Earth and Planetary*  
 457 *Science Letters*. 215, 27–42

458 Busigny, V., Cartigny, P., Philippot, P. 2011. Nitrogen isotopes in ophiolitic metagabbros: A re-  
 459 evaluation of modern nitrogen fluxes in subduction zones and implication for the early Earth  
 460 atmosphere. *Geochimica et Cosmochimica Acta* 75, 7502–7521.

461 Busigny, V., Lebeau, O., Ader, M., Krapez, B., Bekker, A. 2013. Nitrogen cycle in the late archaean  
 462 ferruginous ocean. *Chemical Geology*, 362 115–130

463 Canil, D., Virgo, D., Scarfe, C.M. 1990. Oxidation state of mantle xenoliths from British Columbia,  
 464 Canada. *Contributions to Mineralogy and Petrology*, 104, 453–62

465 Cartigny, P., Boyd, S.R., Harris, J.W., Javoy, M. 1997. Nitrogen isotopes in peridotitic diamonds  
 466 from Fuxian, China: the mantle signature. *Terra Nova*, 9, 175–179

467 Cartigny, P., Harris, J.W., Javoy, M. 1998. Eclogitic Diamond Formation at Jwaneng: No room for a  
 468 recycled component. *Science*, 280, 1421–1424

469 Cottrell, E., Kelley, K.A. 2013. Redox heterogeneity in mid-ocean ridge basalts as a function of  
 470 mantle source. *Science*, 340, 1314–1317

471 Dauphas, N., Marty, B. 1999. Heavy nitrogen in carbonatites of the Kola Peninsula: A possible  
 472 signature of the deep mantle. *Science*, 286, 2488–2490

473 Dobrzhenetskaya, L.F., Wirth, R., Yang, J., Hutcheon, I.D., Weber, P.K., Green, H.W. 2009. High-  
 474 pressure highly reduced nitrides and oxides from chromitite of a Tibetan ophiolite. *Proceedings of*  
 475 *the National Academy of Sciences*, 106, 19233–19238

476 Elkins, L.J., Fischer, T.P., Hilton, D.R., Sharp, Z.D., McKnight, S., Walker, J. 2006. Tracing nitrogen in  
 477 volcanic and geothermal volatiles from the Nicaraguan volcanic front. *Geochimica et*  
 478 *Cosmochimica Acta*. 70, 5215–5235

479 Facq, S., Daniel, I., Sverjensky, D. A. 2014. *In situ* Raman study and thermodynamic model of  
 480 aqueous carbonate speciation in equilibrium with aragonite under subduction zone conditions.  
 481 *Geochim. Cosmochim. Acta*, 132, 375–390

482 Fischer, T.P., Hilton, D.R., Zimmer, M.M, Shaw, A.M., Sharp, Z.D., Walker, J.A. 2002. Subduction  
 483 and recycling of nitrogen along the Central American margin. *Science*, 297, 1154–1157

484 Fischer, T.P., Takahata, N., Sano, Y., Sumino, H., Hilton, D.R., 2005. Nitrogen isotopes of the  
 485 mantle: insights from mineral separates. *Geophysical Research Letters*. 32.  
 486 doi:10.1029/2005GL022792

487 Frost, D.J., McCammon, C.M. 2008. The Redox State of Earth's Mantle. Annual Reviews in Earth  
488 and Planetary Sciences, 36, 389–420

489 Frost, D.J., Liebske, C., Langenhorst, F., McCammon, C.A., Trønnnes, R.G. 2004. Experimental  
490 evidence for the existence of iron-rich metal in the Earth's lower mantle. *Nature* 248:409–12

491 Frost, D.J., Mann, U., Asahara, Y., Rubie, D.C. 2008. The redox state of the mantle during and just  
492 after core formation. *Phil. Trans. R. Soc. A*, 366, 4315–4337

493 Galvez, M.E., Connolly, J.A.D., Manning, C.E. 2016. Implications for metal and volatile cycles from  
494 the pH of subduction zone fluids. *Nature*. 539, 420–424

495 Grove, T.L., Chatterjee, N., Parman, S.W., Medard, E. 2006. The influence of H<sub>2</sub>O on mantle wedge  
496 melting. *Earth and Planetary Science Letters*. 249, 74–89

497 Haendel, D., Muhle, K., Nitzsche, H.M., Stiehl, G., Wand, U. 1986. Isotopic variations of the fixed  
498 nitrogen in metamorphic rocks. *Geochim. Cosmochim. Acta*, 50, 749–758

499 Halama, R., Bebout, G., John, T., Scambelluri, M. 2014. Nitrogen recycling in subducted mantle  
500 rocks and implications for the global nitrogen cycle. *Int. J. Earth Sci.* 103: 2081–2099

501 Halama, R., Bebout, G.E., John, T., Schenk, V. 2010. Nitrogen recycling in subducted oceanic  
502 lithosphere: The record in high-and ultrahigh-pressure metabasaltic rocks. *Geochimica et*  
503 *Cosmochimica Acta*. 74, 1636–1652

504 Hanschmann G. 1981. Berechnung von Isotopieeffekten auf quantenchemischer Grundlage am  
505 Beispiel stickstoffhaltiger Moleküle. *ZFI Mitteilungen* 41, 19–31

506 Harlow, G.E., Davis, R. 2004. Status report on stability of K-rich phases at mantle conditions.  
507 *Lithos*, 77, 647–653

508 Helgeson H. C., Kirkham D. H. 1974a. Theoretical prediction of the thermodynamic behavior of  
509 aqueous electrolytes at high pressures and temperatures: I. Summary of the  
510 thermodynamic/electrostatic properties of the solvent. *Am. J. Sci.* 274, 1089–1198.

511 Helgeson H. C., Kirkham D. H. 1974b. Theoretical prediction of the thermodynamic behavior of  
512 aqueous electrolytes at high pressures and temperatures: II. Debye–Hückel parameters for activity  
513 coefficients and relative partial molal properties. *Am. J. Sci.* 274, 1199–1261.

514 Helgeson H. C., Kirkham D. H. 1976. Theoretical prediction of the thermodynamic properties of  
515 aqueous electrolytes at high pressures and temperatures. III. Equation of state for aqueous  
516 species at infinite dilution. *Am. J. Sci.* 276, 97–240.

517 Helgeson H. C., Kirkham D. H., Flowers G. C. 1981. Theoretical prediction of the thermodynamic  
518 behavior of aqueous electrolytes at high pressures and temperatures. IV. Calculation of activity  
519 coefficients, osmotic coefficients, and apparent molal and standard and relative partial molal  
520 properties to 5 kb and 600 C. *Am. J. Sci.* 281, 1241–1516.

521 Herd, C.D.K. 2008. Basalts as probes of planetary interior redox state. In *Oxygen in the Solar*  
522 *System* (eds. G. J. MacPherson, D. W. Mittlefehldt and J. H. Jones). Mineralogical Society of  
523 America, Chantilly, VA.

524 Honma, H., Itihara, Y. 1983. Distribution of ammonium in minerals of metamorphic and granitic  
525 rocks. *Geochim. Cosmochim. Acta*, 45, 983–988

526 Ionov D.A, Wood B.J. 1992. The oxidation state of subcontinental mantle: oxygen  
527 thermobarometry of mantle xenoliths from central Asia. *Contrib. Mineral. Petrol.* 111:179–93

528 Johnson, B., Goldblatt, C. 2015. The nitrogen budget of Earth. *Earth-Science Reviews* 148, 150–173



529 Johnson J. W., Oelkers E. H., Helgeson H. C. 1992. SUPCRT92: a software package for calculating  
 530 the standard molal thermodynamic properties of minerals, gases, aqueous species, and reactions  
 531 from 1 to 5000 bars and 0 to 1000 C. *Comput. Geosci.* 18, 899–947

532 Lécuyer, C., Ricard, Y. 1999. Long-term fluxes and budget of ferric iron: implication for the redox  
 533 states of the Earth's mantle and atmosphere. *Earth Planet. Sci. Lett.* 165:197–211

534 Li, Y., Keppler, H. 2014. Nitrogen speciation in mantle and crustal fluids. *Geochimica Cosmochimica*  
 535 *et Acta*, 129, 13–32

536 Li, Y., Wiedenbeck, M., Shcheka, S., Keppler, H. 2013. Nitrogen solubility in upper mantle minerals.  
 537 *Earth Planetary Science Letters.* 377, 311–323

538 Lyons, T.W., Reinhard, C.T., Planavsky, N.J. 2014. The rise of oxygen in Earth's early ocean and  
 539 atmosphere. *Nature.* 506, 307-315

540 Marty, B., Dauphas, N. 2003. The nitrogen record of crust-mantle interaction and mantle  
 541 convection from Archean to present. *Earth Planet. Sci. Lett.*, 206, 397–410

542 Marty, B., Zimmermann, L., Pujol, M., Burgess, R., Philippot, P. 2013. Nitrogen isotopic  
 543 composition and density of the Archean atmosphere. *Science*, 342, 101–104

544 Marty, B. 1995. Nitrogen content of the mantle inferred from N<sub>2</sub>-Ar correlation in oceanic basalts.  
 545 *Nature*, 377, 326–329

546 Migdisov A.A., Williams-Jones A.E., Wagner T. 2009. An experimental study of the solubility and  
 547 speciation of the Rare Earth Elements (III) in fluoride- and chloride-bearing aqueous solutions at  
 548 temperatures up to 300 °C. *Geochimica et Cosmochimica Acta*, 73, 7087-7109

549 Mikhail, S. Sverjensky, D.A. 2014. Nitrogen speciation in upper mantle fluids and the origin of  
 550 Earth's nitrogen-rich atmosphere. *Nature. Geoscience* 7, 816–819

551 Mikhail, S., Verchovsky, A.B., Howell, D., Hutchison, M.T., Southworth, R., Thomson, A.R.,  
 552 Warburton, P., Jones, A.P., and Milledge, H.J. 2014. Constraining the internal variability of the  
 553 stable isotopes of carbon and nitrogen within mantle diamonds. *Chemical Geology*, 366, 14–23

554 Mohapatra, R., Harrison, D., Ott, U., Gilmour, J., Trierloff, M. 2009. Noble gas and nitrogen isotopic  
 555 components in Oceanic Island Basalts. *Chemical Geology*, 266, 29–37

556 Palot, M., Cartigny, P., Harris, J.W., Kaminsky, F.V., Stachel, T., 2012. Evidence for deep mantle  
 557 convection and primordial heterogeneity from nitrogen and carbon stable isotopes in diamond.  
 558 *Earth Planet. Sci. Lett.* 357–358, 179–193

559 Palya, A.P., Buick, I.S., Bebout, G.E. 2011. Storage and mobility of nitrogen in the continental crust:  
 560 Evidence from partially melted metasedimentary rocks, Mt. Stafford, Australia. *Chem. Geol.*, 281,  
 561 211–226

562 Pan, D., Spanu, L., Harrison, B., Sverjensky, D.A., Galli, G. 2013. The dielectric constant of water  
 563 under extreme conditions and transport of carbonates in the deep Earth. *Proc. Nat. Acad. Sci.* 110,  
 564 6646–6650

565 Parkinson, I.J. Arculus, R.J. 1999. The redox state of subduction zones: insights from arc-  
 566 peridotites. *Chem. Geol.* 160, 409–423

567 Rohrbach, A., Ballhaus, C., Golla-Schindler, U., Ulmer, P., Kamenetsky, V.S., Kuzmin, D.V. 2007.  
 568 Metal saturation in the upper mantle. *Nature*, 449, 456–458.

569 Shock, E.L., Oelkers, E.H., Johnson, J.W., Sverjensky, D.A., Helgeson, H.C. 1992. Calculation of the  
570 thermodynamic and transport properties of aqueous species at high pressures and temperatures:  
571 effective electrostatic radii to 1000 C and 5 kb. *Faraday Soc. Trans.* 88, 803–826

572 Shock, E.L., Helgeson, H.C. 1988. Calculation of the thermodynamic and transport properties of  
573 aqueous species at high pressures and temperatures: Correlation algorithms for ionic aqueous  
574 species and equation of state predictions to 5 kb and 1000 °C. *Geochimica et Cosmochimica Acta*  
575 52: 2009-2036.

576 Simakov, S.R. 2006. Redox state and peridotites from sub-cratonic upper mantle and a connection  
577 with diamond genesis. *Contrib Mineral Petrol.*, 151, 282–296

578 Sleep, N.H., Windley, B.F. 1982. Archean plate tectonics: constraints and inferences. *Journal of*  
579 *Geology*. 90, 363–379

580 Smart, K.S., Chacko, T., Stachel, T., Muehlenbachs, K., Stern, R.A., Heaman, L.M. 2011. Diamond  
581 growth from oxidized carbon sources beneath the Northern Slave Craton, Canada: a  $\delta^{13}\text{C}$ -N study  
582 of eclogite-hosted diamonds from the Jericho kimberlite. *Geochimica et Cosmochimica Acta*. 75,  
583 6027-6047

584 Smart, K.S., Tappe, S., Simonetti, A., Simonetti, S.S., Woodland, A.B., Harris, C. *In Press*. Tectonic  
585 significance and redox state of Paleoproterozoic eclogite and pyroxenite components in the Slave  
586 cratonic mantle lithosphere, Voyageur kimberlite, Arctic Canada. *Chemical Geology*. DOI:  
587 <http://dx.doi.org/10.1016/j.chemgeo.2016.10.014>

588 Smith, E.M., Kopylova, M.G., Frezzotti, M.L., and Afanasiev, V.P. 2014. N-rich fluid inclusions in  
589 octahedrally-grown diamond. *Earth and Planetary Science Letters*, 393, 39–48

590 Som, S.M., Buick, R., Hagadorn, J.W., Blake, T.S., Perreault, J.M., Harnmeijer, J.P., Catling, D.C.  
591 2016. Earth's air pressure 2.7 billion years ago constrained to less than half of modern levels.  
592 *Nature Geosci.*, advance online publication.

593 Som, S.M., Catling, D.C., Harnmeijer, J.P., Polivka, P.M., Buick, R. 2012. Air density 2.7 billion years  
594 ago limited to less than twice modern levels by fossil raindrop imprints. *Nature*, 484, 359-362.

595 Stagno, V., Frost, D.J., McCammon, C.A., Mohseni, H., Fei, Y. 2015. The oxygen fugacity at which  
596 graphite or diamond forms from carbonate-bearing melts in eclogitic rocks. *Contrib. Mineral.*  
597 *Petrol.*, 169, 16

598 Stüeken, E.A., Kipp, M.A., Koehler, M.C., Buick, R. 2016. The evolution of Earth's biogeochemical  
599 nitrogen cycle. *Earth-Science Reviews*, 160, 220–239

600 Sverjensky, D.A., Huang, F. 2015. Diamond formation due to a pH drop during fluid–rock  
601 interactions. *Nature Communications*, 6, 8702

602 Sverjensky, D.A., Harrison, B., Azzolini, D. 2014. Water in the deep Earth: The dielectric constant  
603 and the solubilities of quartz and corundum to 60 kb and 1,200 °C. *Geochim. Cosmochim. Acta*  
604 129, 125–145

605 Sverjensky, D.A., Stagno, V., Huang, F. 2014. Important role for organic carbon in subduction-zone  
606 fluids in the deep carbon cycle. *Nat. Geosci.* 7, 909–913

607 Syracuse, E.M., van Keken, P.E., Abers, G.A. 2010. The global range of subduction zone thermal  
608 models, *Phys. Earth Planet. Inter.*, 51, 1761–1782

609 Tanger, J.C., Helgeson H.C. 1988. Calculation of the thermodynamic and transport properties of  
610 aqueous species at high pressures and temperatures: Revised equations of state for the standard  
611 partial molal properties of ions and electrolytes. *Amer. J. Sci.* 288: 19-98.

- 612 Wade, J., Wood, B.J. 2005. Core formation and the oxidation state of the Earth. *Earth Planet. Sci.*  
613 *Lett.* 236, 78–95
- 614 Watenphul, A., Wunder, B., Wirth, R., Heinrich, W., 2010. Ammonium-bearing clinopyroxene: a  
615 potential nitrogen reservoir in the Earth's mantle. *Chem. Geol.* 270, 240–248
- 616 Williams-Jones, A.E., Migdisov, A.A., Samson, I.M. 2012. Hydrothermal Mobilization of the Rare  
617 Earth Elements – a Tale of “Ceria” and “Yttria”. *Elements*, 8, 355–360
- 618 Wood, B.J., Virgo, D. 1989. Upper mantle oxidation state: ferric iron contents of lherzolite spinels  
619 by  $^{57}\text{Fe}$  Mössbauer spectroscopy and resultant oxygen fugacities. *Geochim Cosmochim Acta* 53,  
620 1277–1291
- 621 Wood, B.J., Bryndzia, L.T., Johnson, K.E. 1990. Mantle oxidation state and its relationship to  
622 tectonic environment and fluid speciation. *Science*, 248, 337–345
- 623 Wood, B.J., Walter, M.J., Wade, J. 2006. Accretion of the Earth and segregation of its core. *Nature*.  
624 441, 825–833
- 625 Woodland, A.B., Kornprobst, J., Wood, B.J. 1992. Oxygen thermobarometry of orogenic lherzolite  
626 massifs. *J Petrol*, 33, 203–230
- 627 Woodland, A.B., Kornprobst, J., McPherson, E., Bodinier, J-L., Menzies, M.A., 1996. Metasomatic  
628 interactions in the lithospheric mantle. Petrologic evidence from the Lherz massif, French  
629 Pyrenees. *Chem. Geol.* 134, 83–112
- 630 Woodland, A.B., Kornprobst, J., Tabit, A. 2006. Ferric iron in orogenic lherzolite massifs and  
631 controls of oxygen fugacity in the upper mantle. *Lithos*, 89, 222–241
- 632 Yokochi, R., Marty, B., Chazot, G., Burnard, P., 2009. Nitrogen in peridotite xenoliths: lithophile  
633 behaviour and magmatic isotope fractionation. *Geochim. Cosmochim. Acta* 73, 4843–4861
- 634 Zhang, C., Duan, Z.A. 2009. A model for C–O–H fluid in the Earth’s mantle. *Geochim. Cosmochim.*  
635 *Acta*, 73, 2089–2102

636

## 637 **Figures:**

638 **Figure 1:** Calculated  $\log f\text{O}_2$ -pH diagrams for nitrogen speciation in supercritical aqueous fluids  
639 using the Deep Earth Water (DEW) model (see methods). The colored boxes show where  
640 predicted compositions of upper mantle (peridotite; green), mantle wedge (arc peridotite; blue)  
641 and subducted oceanic crust (eclogite; orange) are predicted to plot under these  $f\text{O}_2$  – pH  
642 conditions. The boundaries between nitrogen-species represent a range of total dissolved  
643 nitrogen. For the purposes of examining nitrogen speciation under redox conditions appropriate  
644 to silicate mantles with a peridotitic bulk composition, we have expressed the  $\log f\text{O}_2$  relative to  
645 the quartz-fayalite-magnetite mineral buffer (expressed as  $\Delta\text{QFM}$  in log units). The range of  $f\text{O}_2$   
646 values for eclogites shown above represents the global range, and is not intended to represent  
647 any single geographical locality The fields for the oxidation state of peridotitic mantle domains and  
648 eclogitic mantle domains are described in the text. The pH values represent the equilibrium with  
649 jadeite + kyanite +  $\text{SiO}_2$  and a range of total dissolved Mg concentrations (see methods).

650 **Figure 2:** Aqueous speciation of nitrogen in fluids in equilibrium with a model eclogite-facies  
651 mineral assemblages at 5 GPa, and QFM -2, and temperatures ranging from cold to hot subduction  
652 zone conditions. (a) Jadeite + Pyrope + Kyanite + diamond in equilibrium with  
653 fluid containing 0.001 m N, and (b) Jadeite + Pyrope + Kyanite + diamond in equilibrium with  
654 fluid containing 0.1 m N.

655 **Figure 3:** Aqueous speciation of nitrogen in fluids in equilibrium with a model peridotite mineral  
656 assemblages at 5 GPa, QFM -2, and temperatures ranging from cold to hot subduction zone  
657 conditions. (a) Forsterite + Enstatite + Pyrope/Clinocllore + diamond in equilibrium with  
658 fluid containing 0.001 m N, and (b) Forsterite + Enstatite + Pyrope/Clinocllore + diamond in  
659 equilibrium with fluid containing 0.1 m N. Note, the minerals are pyrope at 800 °C and above,  
660 clinocllore at 600 and 700 °C (data from Mikhail & Sverjensky, 2014).

661 **Figure 4:** A cartoon showing the likely pathways followed by nitrogen during subduction. This  
662 cartoon illustrates that there are two options for nitrogen, degassing of neutrally charged  $\text{NH}_3^0$   
663 and  $\text{N}_2^0$ , or re-gassing of the mantle with lattice-bound  $\text{NH}_4^+$  transported by the mineralogical  
664 conveyor belt of K-bearing minerals shown as colored arrows (phengite, phlogopite, K-bearing  
665 clinopyroxene, Phase-X and K-Hollandite). The depth-related stability for the K-bearing phases  
666 shown were taken from Harlow and Davies (2004).